Optimisation of tensile and compressive behaviour of PLA 3D printed parts using categorical response surface methodology

Muhammad Waseem

Department of Industrial Engineering,
University of Engineering and Technology,
Peshawar, Pakistan
Email: mw9722299@gmail.com

Tufail Habib

Department of Industrial Engineering,
University of Engineering and Technology,
Jalozai Campus, Pakistan
Email: tufailh@uetpeshawar.edu.pk

Usman Ghani

Department of Mechanical Engineering,
University of Engineering and Technology,
Jalozai Campus, Pakistan
Email: usmanghani@uetpeshawar.edu.pk

Muhammad Abas*

Department of Industrial Engineering,
University of Engineering and Technology,
Peshawar, Pakistan
Email: muhammadabas@uetpeshawar.edu.pk
*Corresponding author

Qazi Muhammad Usman Jan

Department of Industrial Engineering,
College of Aeronautical Engineering,
National University of Science and Technology,
Islamabad, Pakistan
Email: usmankazi999@gmail.com

Muhammad Alam Zaib Khan

Department of Mechanical Engineering,
University of Engineering and Technology,
Peshawar, Pakistan
Email: alamzaibkhan@uetpeshawar.edu.pk

Abstract: The present study aims to optimise process parameters of 3-D printed polylactic acid (PLA) part using response surface methodology (RSM). The input printing process parameters considered are layer height (*L*), infill percentage (*I*), raster width (*R*) and infill patterns (*P*) (i.e., linear, hexagonal and diamond), while the responses are tensile and compressive strengths. Box Behnken array design is applied for experimental runs and also to fit quadratic regression models. The results revealed that significant parameters affecting compression strength performance are *I*, I^2, *R*, and interaction of *I* and *R*, for tensile strength, are *L*, *I*, I^2, *R*, *P*, and interaction of *P* with *L* and *I*. The simultaneously optimised parameters obtained based on composite desirability function for compression and tensile strength are *L* = 0.1 mm, *I* = 100%, *R* = 0.4 mm, and *P* = hexagonal, while the obtained maximum compression and tensile strength are 9.06 kN and 1.67 kN.

Keywords: additive manufacturing; fused deposition modelling; FDM; polylactic acid; PLA; tensile strength; compression strength; response surface methodology; RSM.

Reference to this paper should be made as follows: Waseem, M., Habib, T., Ghani, U., Abas, M., Jan, Q.M.U. and Khan, M.A.Z. (2022) 'Optimisation of tensile and compressive behaviour of PLA 3D printed parts using categorical response surface methodology', *Int. J. Industrial and Systems Engineering*, Vol. 41, No. 4, pp.417–437.

Biographical notes: Muhammad Waseem is a Laboratory Engineer at the University of Engineering and Technology (UET), Peshawar, Pakistan. He received his Master's degree in Industrial Engineering from the University of Engineering and Technology, Peshawar, Pakistan in 2019, and a Bachelor's degree in Industrial Engineering from the same institute in 2017. His research interest includes production optimisation, additive manufacturing, and modelling and simulation.

Tufail Habib is an Assistant Professor at Industrial Department at UET Peshawar, Pakistan. He completed his PhD in Industrial Engineering in 2014 from Aalborg University Denmark, MS degree in Mechatronics from FH Aachen Germany, and BSc Engineering degree from UET, Peshawar. His areas of interest are advance manufacturing processes, mass customisation, product innovation and Industry 4.0.

Usman Ghani is working as an Assistant Professor in the Department of Mechanical Engineering UET Peshawar. His speciality is in the manufacturing system design and planning and technology business models. He is active member of British Engineering Council and member of IMechE.

Muhammad Abas is a Lecturer at Department of Industrial Engineering at UET Peshawar, Pakistan. He completed his MS in Mechanical Engineering in 2016 from GIK Institute, Topi, Pakistan, and BSc in Industrial Engineering from UET, Peshawar in 2013. His areas of interest are additive manufacturing, machining optimisation, and construction management.

Qazi Muhammad Usman Jan is a Laboratory Engineer at the National University of Sciences and Technology (NUST), Islamabad, Pakistan. He received his Master's degree in Industrial Engineering from the University of Engineering and Technology, Peshawar, Pakistan in 2019, and a Bachelor's degree in Industrial Engineering from the same institute in 2015. His research interest includes production optimisation, additive manufacturing, and modelling and simulation.

Muhammad Alam Zaib Khan is an Assistant Professor at Mechanical Engineering Department at UET Peshawar, Pakistan. He completed his PhD and MS in Automotive Engineering from Loughborough University, UK, and BSc Mechanical Engineering degree from UET, Peshawar. His research interests are design and analysis of experiments power plant design and applied thermodynamics.

1 Introduction

The application of additive manufacturing (AM) is becoming a reality that can fabricate complex geometries with less time. Nowadays, the industries, namely the automotive industry, aerospace engineering, bioengineering, and medical fields, are adopting it progressively. AM employs several methods to fabricate a part, depending upon the nature of raw material. Fused deposition modelling (FDM), stereolithography (STL), direct metal deposition (DMD), selective laser sintering (SLS), and inkjet modelling (IJM) are some of the technologies that are widely used in AM (Mohamed et al., 2015). These technologies are mainly differed by types of processing materials and methods of material transformation. Although all these technologies have a wide range of applications in various sectors, FDM is leading in the market as it has accounted for nearly half of the number of machines on the market (Mohamed et al., 2015). FDM uses a filament polymer that is fed into the extruder, where it is melted by the heaters and extrudes out of the nozzle. The motion of the extruder is controlled from a computer or built-in controller in the machine (Bellehumeur et al., 2004). FDM uses several materials to print the parts, including acrylonitrile butadiene styrene (ABS), polylactic acid (PLA), polycarbonate (PC), polystyrene and nylon. ABS and PLA are the most commonly used materials in FDM. Although PLA has low strength as compared to ABS, it has the benefits of its biodegradable nature.

Strength, cost, and time to build are the significant factors that every manufacturer and customer demand in FDM (Haleem et al., 2020). The requirement to manufacture a quality product at a low cost is a challenge to the researchers in this FDM field (Izdebska and Thomas, 2016). The researchers are studying the parameters and have developed several solutions to improve the quality. Different parameters like layer thickness, infill percentage, infill patterns, and orientation have been studied, and various combinations are designed to get better results (Trhlíková et al., 2016; Luzanin et al., 2014; Bagsik et al., 2010). Wang et al. (2007) optimised the tensile strength, surface roughness, and dimensional accuracy of ABS parts by analysing the input parameters (Kumar et al., 2020; Shandilya et al., 2012). Zhang and Peng (2012) used the Taguchi method with a fuzzy comprehensive evaluation to examine the impact of layer thickness, extrusion velocity, and filling velocity on the deformation of ABS parts. Sood et al. (2010) used

central composite design (CCD), to investigate the significance of raster angle and layer thickness on deformation and residual stresses. Rayegani and Onwubolu (2014) obtained optimum parametric setting for the air gap, raster angle, build orientation, and width to achieve maximum tensile strength by using full factorial design. Hossain et al. (2014) studied the impact of input process parameters on the young's modulus, ultimate tensile strength, and strain. They found air gap removal as a significant factor. Peng et al. (2014) analysed the effects of extrusion, filling velocity and layer thickness on manufacturing efficiency and accuracy.

In comparison to injection moulding, the proper selection of FDM parameters can achieve better mechanical properties. The results are comparatively better than the injection moulded parts (Dawoud et al., 2016). Torres et al. (2016) investigated the effect of printing speed and layer height on PLA prototypes. Decreasing the speed and lowering the layer height improved the surface quality. Panda et al. (2017) used the evolutionary system identification method and concluded that dimensional error is mostly affected by filling velocity and line width compensation.

The challenge of 3D printing technology is the possibility of making a prototype to redesign a product quickly, firmly, and cheaply (Izdebska and Thomas, 2016). Much research has been carried out regarding the performance of FDM technology by investigation of the process parameters to evaluate the impact on mechanical properties. The governing printing parameters involved are nozzle temperature, layer thickness, percentage infill, raster orientation, and extrusion width (Trhlíková et al., 2016; Luzanin et al., 2014; Bagsik et al., 2010; Patel et al., 2015). The Taguchi's design matrix, signal to noise ratio (S/N) and analysis of variance (ANOVA) were commonly utilised to optimise the printing parameters of FDM. However, at present, there are few studies on the performance of a low-cost 3D printer regarding mechanical properties. Recently, research on evaluation on the mechanical properties using MakerBot Replicator 2 Desktop 3D printer has been done by manipulating layer thickness, percent infill, and print orientation (Melenka et al., 2015). Tymark et al. (2014) conducted a study on the tensile strength and elastic modulus of printed products using normal environmental conditions for general users of open-source 3D printers. These results indicate that the parts that are removed or subtracted during the printing process by Reprap 3D printers have cheaper production process costs. Fernandez-Vicente et al. (2016) conducted a study on the influence of infill parameters on tensile strength in 3D printing products. The results showed that at the same density, the honeycomb pattern (honeycomb) had better tensile strength, although the difference between the pattern parameters was less than 5%. This difference can be due to the variation in the number of extruded plastics for each pattern. In such cases, it may explain the cause of the difference in the modulus of elasticity. Sukindar et al. (2017) conducted a study using open source 3D printers developed by Repetier-Host software with PLA materials and three-level variations for three parameters, including layer thickness, shell thickness, and print speed. Results from ANOVA showed that shell thickness had a significant effect on influencing tensile strength test results. Also by increasing the thickness of the shell from 0.4 mm to 1.2 mm increases the tensile strength of the specimen. Table 1 summarised the various researches carried out on the process parameters optimisation of FDM through different optimisation techniques for different materials under different printing process parameters.

Table 1 Overview of studies by applying different optimisation techniques in FDM technology

Study	*Parameters*		*Material*	*Optimisation technique*
	Input	*Output*		
Abid et al. (2019)	Manufacturing direction, deposition angle	Young modulus, the yield stress, the tensile strength, and the deformation at fracture in tension	ABS	RSM
Camargo et al. (2019)	Infill and layer thickness	Mechanical properties tensile strength, flexural strength, and impact energy	PLA-graphene	CCD
Rajpurohit and Dave (2020)	Build parameters	Mechanical strength	PLA	ANFIS
Puigoriol-Forcada et al. (2018)	Part build orientation	Flexural fatigue behaviour	Polycarbonate	Experimental
Nugroho and Budiantoro (2019)	Temperatures, extrusion width, infill density, and infill pattern	Tensile strength	PLA	Taguchi method
Kamoona et al. (2018)	Air gap, raster angle, and build orientation	Flexural strength	Nylon	Response surface methodology
Rohde et al. (2018)	Raster angle and build Orientation	Young's modulus and Poisson's ratio, tensile and shear properties	ABS and PC	Experimental study
Equbal et al. (2019)	Layer thickness, orientation, air gap, raster angle, raster width	Dimensional accuracy	ABS	Grey Taguchi method
Kumar et al. (2014)	Layer thickness, contour width, air gap, raster orientation, raster width	Surface roughness	ABS-M30i	Taguchi method and ANOVA procedure
Anitha et al. (2001)	Layer thickness, speed of deposition and road width	Surface roughness	ABS	Taguchi, (S/N) and ANOVA procedure
Zhang and Peng (2012)	Filling velocity, extrusion velocity, wire-width compensation, layer thickness	Dimensional error and warpage deformation	ABS	Taguchi method
Current research	Infill percentage, infill pattern, layer height, raster width	Tensile strength and compression strength	PLA	RSM-Box Behnken

Material is not the only factor contributing to the strength of the printed object. The technology and the parametric setting for part printing also play a significant role. Hence an optimum combination of printing process parameters is necessary to achieve desired results. Therefore this research study focuses on the influence of process parameters, namely layer height, infill percentage, raster width and infill pattern type (linear, hexagonal and diamond) on the mechanical properties, i.e., compression and tensile strength of PLA material by using response surface methodology (RSM). This study is unique as a prediction model is developed to study the relationship between process parameters and responses. Model fitting and ANOVA is used to check the adequacy of the models. In addition to that, the effect of tensile and compression strength values are plotted as surface plots using fitted regression models. Finally, printing process parameters are simultaneously optimised for compression, and tensile strength using composite desirability function, and sensitivity analysis is performed to validate the performance of optimised levels. The novelty of this present research is that no such study has been reported that analyses the simultaneous effect of such combination of process parameters on compression and tensile strength of PLA material using categorical RSM. Finally, the results in the present provide useful technical information on FDM process parameters to improve the compression, and tensile of 3D printed parts.

The rest of this paper is organised as follows: Section 2 describes materials and methods, including experimental setup, experimental design, specimen preparation and 3D printing process parameters. Section 3 describes the results obtained by applying various techniques. Model fitting and ANOVA is used to check the adequacy of the model and validate it before applying the multi-response optimisation. This section also discusses the results obtained in this research. Finally, Section 4 summarises and concludes the paper with prospects as well.

2 Materials and methods

2.1 Experimental setup

In this study, the MakerBot desktop 3D printer (based on FDM) is used to fabricate the PLA specimens. Samples are printed from the continuous supply of PLA filament to the printer. Figure 1(a) shows a schematic arrangement of the printer based on FDM. Figure 1(b) shows the actual printer. The test specimens are printed according to ASTM D-638 and D-695 (Equbal et al., 2019; Kumar et al., 2014) with an extrusion temperature of 240°C, the speed at 130 mm/s, and bed surface temperature at 70°C as shown in Figure 2.

Figure 1 (a) Schematic of FDM (b) Actual setup of FDM (c) Compression specimen while being printed (see online version for colours)

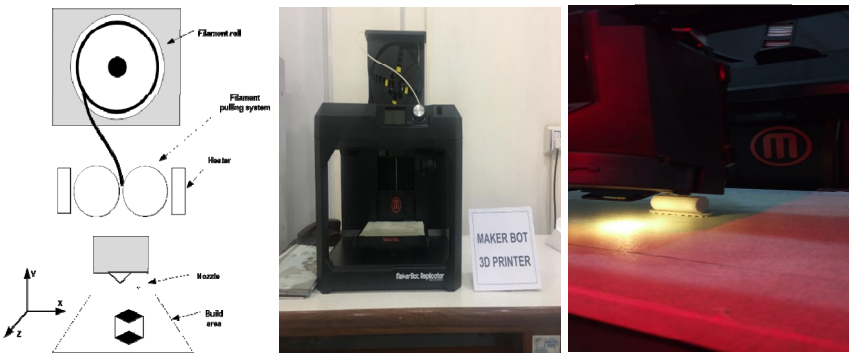

(a) (b) (c)

Figure 2 Test specimen, (a) schematic of the tensile specimen (b) printed tensile specimen (c) schematic of compression specimen (d) printed compression specimen (see online version for colours)

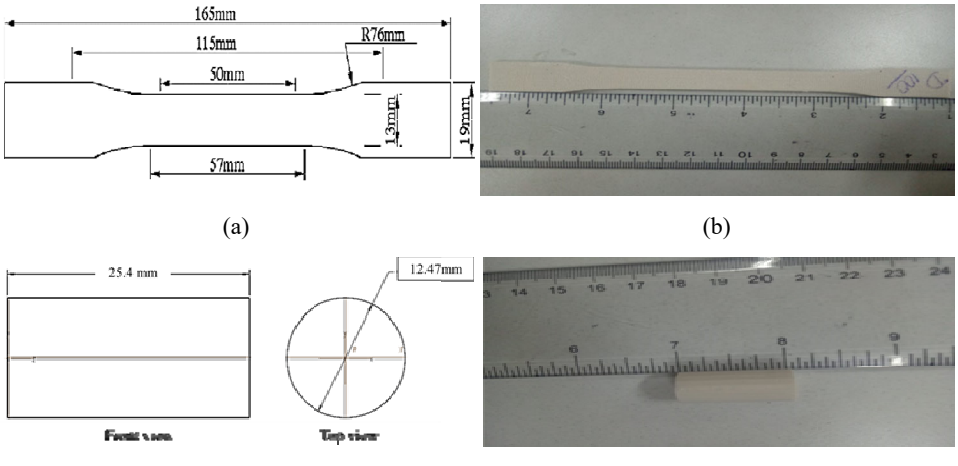

(a) (b)

(c) (d)

2.2 Experimental design

For experimental runs, a Box Behnken design based on RSM is selected. The Box Behnken design is a second-order method based on a three-level factorial design for three and more factors with chosen points from a system structure (Box et al., 1978). The two different forms of this design are:

a cube containing central and middle points at the edges

b three interlocking 22 factorial designs with central points.

The required experimental runs (R) are calculated by $R = 2k(k - 1) + C$, where k is the number of factors, while C is the centre point. The advantage of this design is that it reduces experimental runs and many factors that can be used efficiently in one process. It allows a good estimation of parameters in the quadratic model and much more efficient than CCD and three-level full factorial design (Ferreira et al., 2007; Kumar et al., 2018). The performance of Box Behnken can improve by adjusting the factors at three levels as –1 (lower), 0 (neutral), and +1 (higher).

In the present study, the categorical Box Behnken design is utilised to analyse and optimise process parameters affecting tensile and compressive behaviour of FDM manufactured parts. The parameters considered for the study are one categorical, i.e., infill patterns, i.e., linear, hexagonal, and diamond, while three continuous, i.e., layer height, infill percentage and raster width. Table 2 summarises the factors with their levels. The layer height varied from 0.1 to 0.3 mm, raster width from 0.40 to 0.50, while infill percentage varied from 10 to 100%. Experimenters are performed according to categorical Box Behnken design array, and the desired responses are measured accordingly. The regression models are developed and are evaluated based on ANOVA using the coefficient of determination R^2, adjusted R^2, predicted R^2, residual plots, and F-test. Then the composite desirability function is applied to optimise the multiple responses. Finally, the developed models and optimal levels identified are validated by performing experimental confirmation tests.

Table 2 Factors with their levels

Factors	*Symbols*	*Levels*		
		–1	*0*	*1*
Continuous				
Layer height (mm)	L	0.1	0.2	0.3
Infill percentage	I	10	55	100
Raster width (mm)	R	0.4	0.45	0.50
Categorical		1	2	3
Infill pattern	P	Linear	Hexagonal	Diamond

Figure 3 Infill patterns used in this study are, (a) hexagonal (b) diamond (c) linear

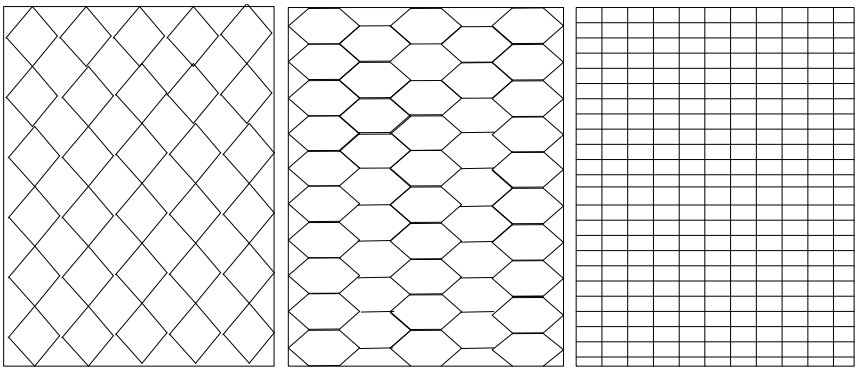

(a) (b) (c)

Figure 3 shows a schematic of infill patterns considered for the study. A total of 45 experiments with coded parameters are conducted based on categorical Box Behnken Design, as shown in Table 3. The purpose of coding the input parameter is to simplify the calculation for regression analysis.

Table 3 Box Behnken design matrix

Coded variables						*Responses*	
StdOrder	*RunOrder*	*Layer height (mm)*	*Infill %age*	*Raster width (mm)*	*Patterns*	*Tensile strength (N)*	*Compressive strength (N)*
1.0	1	–1	–1	0	1	985.6	2,708.1
2.0	2	1	–1	0	1	942.3	2,553.0
18.0	3	–1	1	0	2	1,640.5	8,737.0
9.0	4	0	–1	–1	1	997.8	2,709.5
10.0	5	0	1	–1	1	1,621.4	8,656.0
22.0	6	–1	0	1	2	1,198.7	4,421.3
44.0	7	0	0	0	3	1,180.0	4,242.4
30.0	8	0	0	0	2	1,195.9	4,389.0
31.0	9	–1	–1	0	3	1,106.4	2,589.7
33.0	10	–1	1	0	3	1,655.9	8,609.0
35.0	11	–1	0	–1	3	1,225.3	4,446.7
23.0	12	1	0	1	2	1,190.9	4,399.8
25.0	13	0	1	–1	2	1,624.5	8,765.0
45.0	14	0	0	0	3	1,216.1	4,242.4
38.0	15	1	0	1	3	1,161.7	4,332.5
7.0	16	–1	0	1	1	1,187.3	4,389.4
4.0	17	1	1	0	1	1,475.2	7,502.0
40.0	18	0	1	–1	3	1,654.7	7,503.0
26.0	19	0	–1	1	2	979.8	3,535.0
24.0	20	0	–1	–1	2	988.7	3,715.0
5.0	21	–1	0	–1	1	1,220.7	4,771.3
27.0	22	0	1	1	2	1,577.8	6,434.0
36.0	23	1	0	–1	3	1,167.4	4,319.3
37.0	24	–1	0	1	3	1,161.7	4,301.5
11.0	25	0	–1	1	1	940.1	3,453.0
8.0	26	1	0	1	1	1,103.0	4,213.4
14.0	27	0	0	0	1	1,187.9	4,324.5
20.0	28	–1	0	–1	2	1,208.6	4,669.3
12.0	29	0	1	1	1	1,513.2	6,135.0
43.0	30	0	0	0	3	1,173.7	4,242.4
13.0	31	0	0	0	1	1,201.3	4,324.5
28.0	32	0	0	0	2	1,195.5	4,389.7

Table 3 Box Behnken design matrix (continued)

Coded variables						*Responses*	
StdOrder	*RunOrder*	*Layer height (mm)*	*Infill %age*	*Raster width (mm)*	*Patterns*	*Tensile strength (N)*	*Compressive strength (N)*
21.0	33	1	0	–1	2	1,223.0	4,452.3
16.0	34	–1	–1	0	2	985.6	3,670.0
29.0	35	0	0	0	2	1,197.0	4,447.5
6.0	36	1	0	–1	1	1,089.1	4,413.2
42.0	37	0	1	1	3	1,597.8	6,342.0
19.0	38	1	1	0	2	1,589.0	7,543.0
39	39	0	–1	–1	3	1,113.2	2,589.7
41.0	40	0	–1	1	3	1,098.8	2,595.3
32.0	41	1	–1	0	3	1,101.1	2,657.9
34.0	42	1	1	0	3	1,613.2	7,649.0
17.0	43	1	–1	0	2	979.2	2,593.2
3.0	44	–1	1	0	1	1,579.8	6,776.0
15.0	45	0	0	0	1	1,134.2	4,352.3

Figure 4 UTM used to test the specimens, (a) tensile (b) compression (see online version for colours)

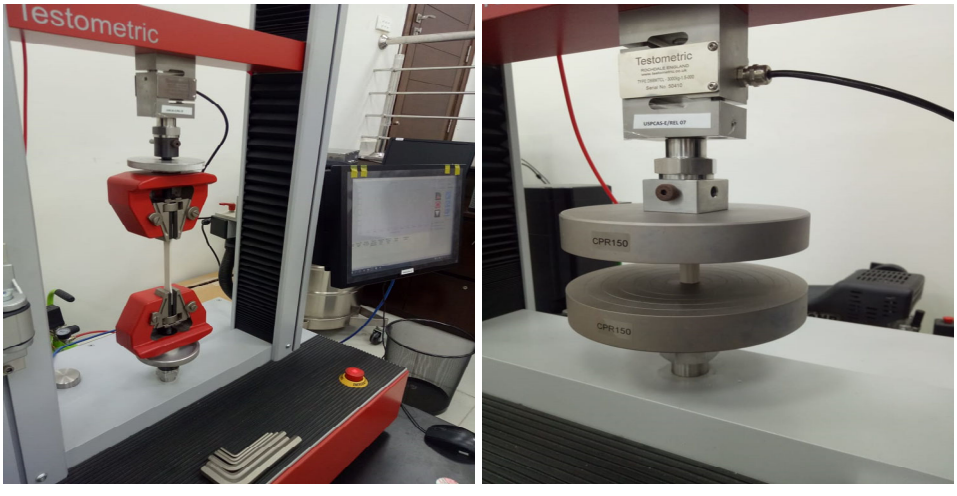

(a) (b)

Each specimen with each combination of process parameters was fabricated and then tested. Instron Testometric universal testing machine (UTM) is used to measure the tensile and compressive strength of the FDM-manufactured parts. Figure 4 shows the arrangements of the equipment and specimen clamping at the two points. The experiments are performed under constant room temperature, i.e., 25°C.

3 Results and discussion

3.1 Model fitting and ANOVA

ANOVA is performed to study the effect of printing parameters on the responses variables and to test the significance and adequacy of regression models. By performing the backward elimination method at an alpha value of 0.1, insignificant model terms are removed from the regression model, and the desired reduced ANOVA with significant terms is shown in Table 4 for compression and tensile strength. It shows that for compression strength infill % (I) and its second-order term (I^2), raster width (R) and interaction of infill % and raster width ($I \times R$) are the most significant model terms with P value less than 0.05. While for tensile strength layer height (L), infill % (I) and its second-order term (I^2), raster width (R), patterns (P), the interaction of layer height and pattern ($L \times P$) and infill % and pattern ($I \times P$) are significant model terms. Additionally, the adequacy measure, i.e., R^2, adjusted R^2 and predicted R^2 for both compression and tensile strength, is closer to 1, so it indicates reasonable agreement and shows the adequacy of models.

Table 4 Reduced ANOVA for compressive strength and tensile strength

Source	*DF*	*Adj SS*	*Adj MS*	*F-Value*	*P-Value*
		Compression strength			
Model	6	142,290,135	23,715,023	130.21	0.000
I	1	127,335,637	127,335,637	699.16	0.000
R	1	1,737,794	1,737,794	9.54	0.004
I^2	1	8,396,875	8,396,875	46.10	0.000
$I \times R$	2	3,610,337	3,610,337	19.82	0.000
Error	38	6,421,827	168,996		
R^2 = 95.36%, adjusted R^2 = 94.63% and predicted R^2 = 93.15%					
		Tensile strength			
Model	10	2,244,922	224,492	215.52	0.000
L	1	11,310	11,310	10.86	0.002
I	1	1,997,805	1,997,805	1,917.94	0.000
R	1	7,477	7,477	7.18	0.011
P	2	36,846	18,423	17.69	0.000
I^2	1	174,654	174,654	167.67	0.000
$L \times P$	2	6,965	3,482	3.34	0.047
$I \times P$	2	9,867	4,933	4.74	0.015
Error	34	35,416	1,042		
R^2 = 98.45%, adjusted R^2 = 97.99% and predicted R^2 = 97.23%					

The prediction models of compression and tensile strength based on categorical Box Behnken design for each infill pattern are expressed in equations (1)–(6). Equations (1)–(3) express prediction model for compression strength, while equations (4)–(6) represents prediction model for tensile strength.

$$Linear = 4,290 + 2,303.4\ I - 269.1\ R + 866\ I^2 - 549\ I \times R \tag{1}$$

$$Hexagonal = 4,616 + 2,303.4\ I - 269.1\ R + 866\ I^2 - 549\ I \times R \tag{2}$$

$$Diamond = 4,249 + 2,303.4\ I - 269.1\ R + 866\ I^2 - 549\ I \times R \tag{3}$$

$$Linear = 1,145.33 - 45.5\ L + 290.5\ I - 17.65\ R + 124.88\ I^2 \tag{4}$$

$$Hexagonal = 1185.05 - 6.4\ L + 312.3\ I - 17.65\ R + 124.88\ I^2 \tag{5}$$

$$Diamond = 1,215.20 - 13.2\ L + 262.8\ I - 17.65\ R + 124.88\ I^2 \tag{6}$$

Figure 5 Residuals plots, (a) normality plot for compression strength (b) normality plot for tensile strength (c) versus fit plot for compression strength (d) versus fit plot for tensile strength (see online version for colours)

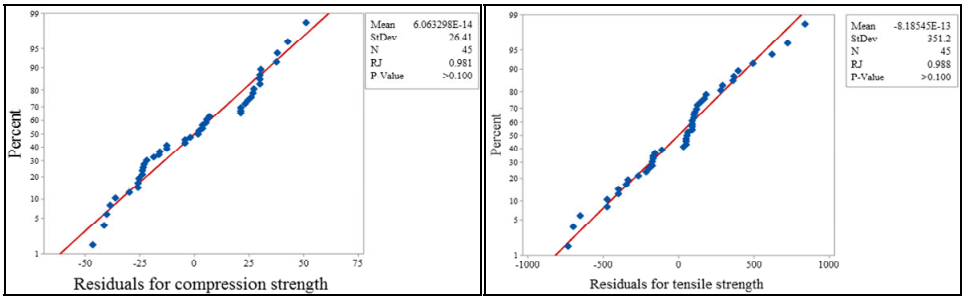

(a) (b)

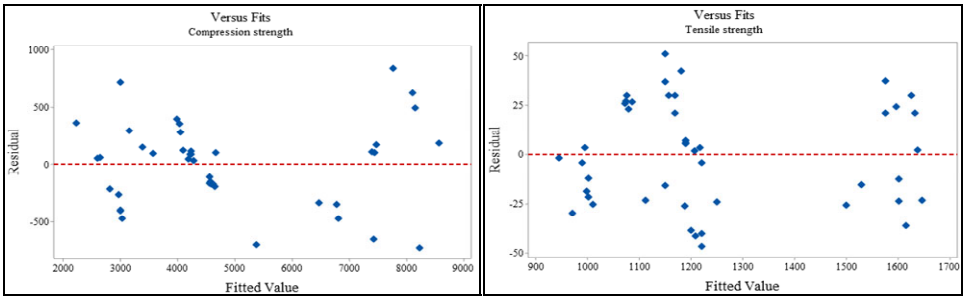

(c) (d)

The adequacy of developed models is further assessed through the assumption of normality of residuals and constant variance. Figures 5(a) and 5(b) shows that residuals for both compression and tensile strength are normally distributed as most of the data points lies near to the fitted line, and *P*-value of Ryan-Joiner (RJ) test are higher than 0.05. Versus fits plots in Figures 5(c) and 5(d) illustrates that residuals for both compression and tensile strength are randomly distributed above and below-fitted line and do not form any sort of increasing or decreasing patterns, so it is assumed that

residuals follow constant variance assumption. From the analysis, it is concluded that developed regression models based on Box Behnken design are adequate and reliable. To validate the performance of regression models, confirmation tests are performed for new experimental runs within range of levels as tabulated in Table 2. Table 5 shows the summarised results of confirmation experiments. The results show that predicted and actual values are in good agreement with a % error of less than 2% for both compression and tensile strength.

Table 5 Confirmation tests for compression and tensile strength

Experiments	*Compression strength (N)*	*Combination of parameters*	*Tensile strength (N)*	*Combination of parameters*
		I-R-P		*L-I-R-P*
		Experiment 1		
Predicted	6,601	100-0.5-diamond	1,598	0.3-100-0.5-hexagonal
Actual	6,696		1,615	
Error%	1.42		1.05	
		Experiment 2		
Predicted	8,277	100-0.4-linear	1,081	0.3-10-0.4-diamond
Actual	8,315		1,101	
Error%	0.46		1.81	
		Experiment 3		
Predicted	2,899	10-0.4-hexagonal	1,588	0.1-100-0.5-linear
Actual	2,913		1,615	
Error%	0.5		1.67	

3.2 Effect of process parameters on compression and tensile strength s 3D surface plots

The effect of process parameters on compression strength (C) is observed in Figure 6 using 3D surface plots for linear, diamond, and hexagonal patterns. Figure 6(a) shows that for linear pattern and diamond pattern having raster angle 0.4 mm, compression strength increases with increase in infill %, i.e., from 10% to 100%. However, shows no increasing or decreasing effect for change in layer height from low level (–1) to a high level (1), i.e., from 0.1 mm to 0.3 mm. For hexagonal pattern decrease in compression strength is observed when layer height increases from low level to a high level as shown in Figure 6(b). From Figure 6(c), it is evident that for linear, hexagonal and diamond patterns at infill % of 100% compression strength decreases with an increase in rater width from low level to a high level, i.e., from 0.40 mm to 0.5 mm. Further, the plots from Figures 6(a) to 6(c) elaborate that higher compression strength can be achieved at a higher level of infill % (i.e., 100%), lower level of layer height and raster width (0.1 mm and 0.4 mm).

Figure 6 3D surface plots show, (a) effect of layer height, infill % linear and diamond patterns on compression strength (b) effect of layer height, infill % hexagonal pattern on compression strength (c) effect of raster width, layer height, linear hexagonal and diamond patterns on compression strength (see online version for colours)

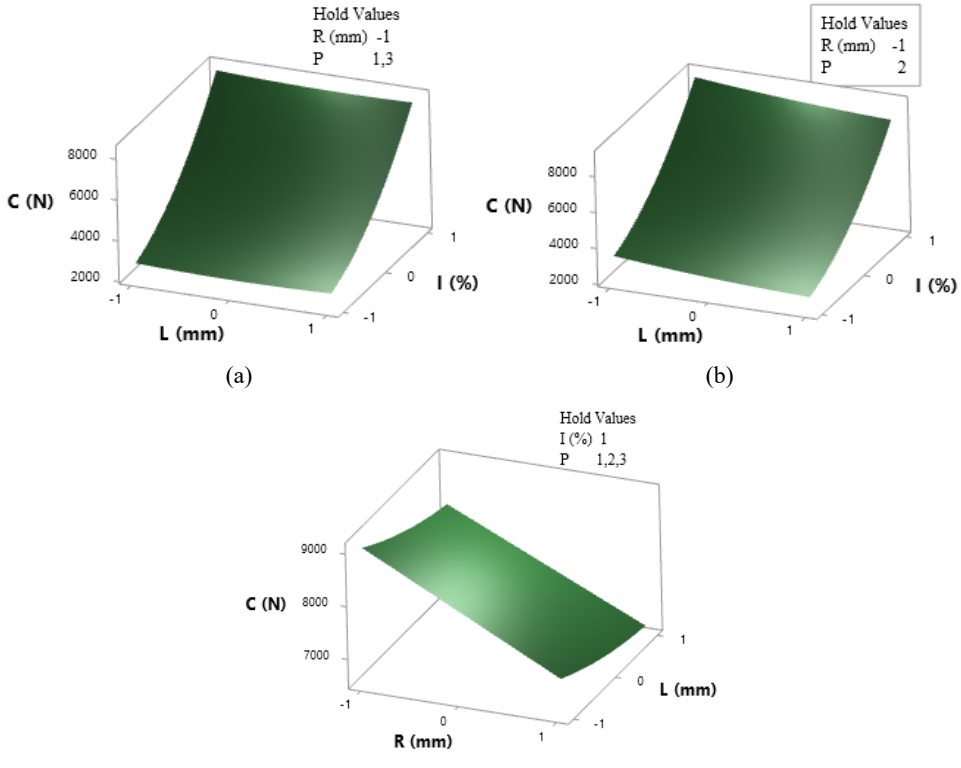

Figure 7 shows the surface plots for tensile strength. Figure 7(a) illustrates that tensile strength decreases with an increase in layer height from low level to a high level, i.e., 0.1 mm to 0.4 mm, however, increases with an increase in infill %, i.e., from 10% to 100%. For diamond and hexagonal patterns with raster width at a lower level, i.e., 0.4 mm layer height have almost no effect on tensile strength while increases with an increase in infill %, as illustrated in Figure 7(b). While the linear, hexagonal and diamond patterns with infill % at a high level (100%), the tensile strength decreases with an increase in raster width from low to a high level (0.4 mm to 0.5 mm), as shown in Figure 7(c). Additionally, the tensile strength plots show that high tensile strength can be achieved at a higher level of infill %, lower level of layer height and raster angle for linear, hexagonal, and diamond patterns.

Figure 7 3D surface plots show, (a) effect of layer height, infill % and linear patterns on tensile strength (b) effect of layer height, infill % hexagonal and diamond pattern on tensile strength (c) effect of raster width, layer height, linear, hexagonal and diamond patterns on tensile strength (see online version for colours)

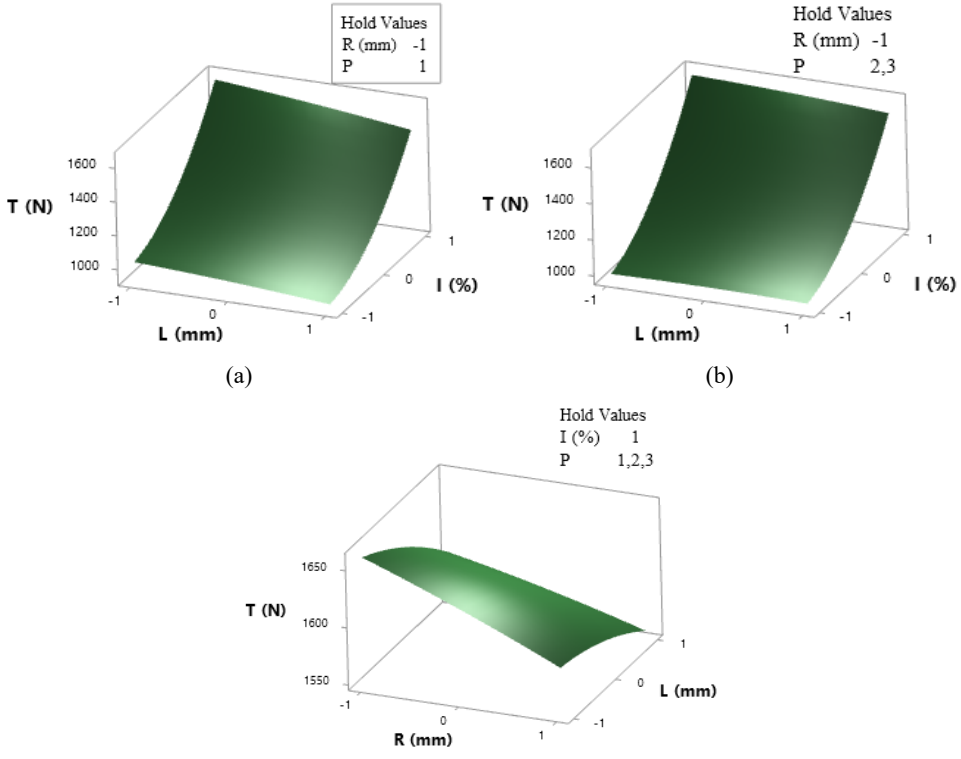

The infill percentage parameter shows a major role in influencing the tensile and compressive strength. The increase of infill percentage increases the density of the material in which more filament to bear the load due to higher mass filament extruded. Yet it affects the period of 3D printing process to produce a stronger product (Popescu et al., 2018). Larger layer height has more mass being extruded resulting in longer time for cooling process. Generally, a larger extrusion tends to produce larger contact areas between layers leading to an increase of bond strength (Murugan et al., 2018). The hexagonal infill pattern has more bonding structure and has a slightly larger density product mass than the others. During the fabrication process, the hexagonal structure expressed of hexagons is carried by forming each hexagon one by one on each layer. On the other hand, to produce the grid (rectangle) and diamond structures, at least two processes are required on each layer to form the structures. It will generate a cooled extrude at a side before it is binding to the other side that leads to a decrease in bonding strength. Therefore, the bonds between the structures being formed of the hexagonal infill pattern are stronger than the others (Nugroho and Budiantoro, 2019).

3.3 Multi response optimisation and sensitivity analysis

The responses, such as tensile and compression strength, are simultaneously optimised by applying composite desirability function using Minitab®19. Desirability values ranges from 0 (undesirable) to 1 (highly desirable) values. Criteria of optimisation for both responses are similar, i.e., to maximise the tensile and compression strength of PLA printed samples. The multi-response optimiser plot obtained using Minitab software is shown in Figure 8. The optimal combination of process parameters to achieve higher tensile and compression strength of PLA printed parts are layer height at a low level (0.1 mm), infill % at a high level (100%), raster width at a low level (0.40 mm). In contrast, the infill pattern type is hexagonal having overall composite desirability value of 1. The optimised compression and tensile strengths obtained are 9,057.11 N and 1,666.283 N, respectively.

Figure 8 Multi-response optimisation plot obtained for tensile and compression phenomena using Minitab software (see online version for colours)

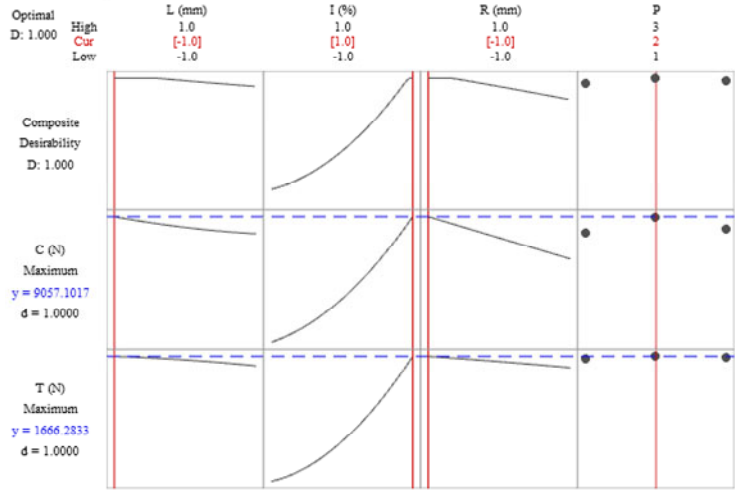

Sensitivity analysis is performed using a response optimiser plot to analyse the effect of changing levels of printing process parameters on compression, and tensile strength of PLA printed parts, as shown in Figure 9. Figure 9(a) shows that by changing the layer height from level –1 (0.2 mm) to level 0 (0.3 mm) and keeping the other parameters at optimal levels the composite desirability value (D) reduces from 1 to 0.979 and the compression and tensile strength decreases from 9,057 N to 8,579 N and 1,666 N to 1,648 N with a percentage reduction of 5.3% in compression strength and 1.1% in tensile strength. Similarly by changing the infill % level from 1 (100%) to 0 (55%), while keeping the other printing parameters at optimal levels composite desirability value reduces considerably from 1 to 0.419, and corresponding decrease in compression and tensile strength from optimal values are 9,057 N to 5,367.9 N (40% reduction in compression strength) and 1,666.3 N to 1,206.84 N (28% reduction in tensile strength). For changing raster width level from –1 (0.4 mm) to 0 (0.45 mm), the desirability values decrease to 0.9343, and the compression and tensile strength along with percentage reduction are 8,111 N (10%) and 1,633 N (28%). Finally, by changing pattern type from

hexagonal to diamond type, the observed change in desirability value is 0.9803, and the corresponding compression and tensile strength with percentage decrease are 8,523 N (6%) and 1,659 N (0.2%). Figure 10 shows a comparison of percentage reduction in compression and tensile strength with changing optimal levels in uncoded form. It shows that compression and tensile strength are significantly affected by changing the optimal values of infill % from 100% to 55% and 10% compare to the changing of other printing parameters namely layer height, raster width and patterns type [linear (*L*), hexagonal (*H*) and diamond (*D*)].

Figure 9 Sensitivity analysis of tensile and compression strength by changing optimal levels, (a) layer height from level –1 to level 0 (b) infill % from level 1 to level 0 (c) raster width from level –1 to 0 (d) infill pattern from hexagonal to diamond (see online version for colours)

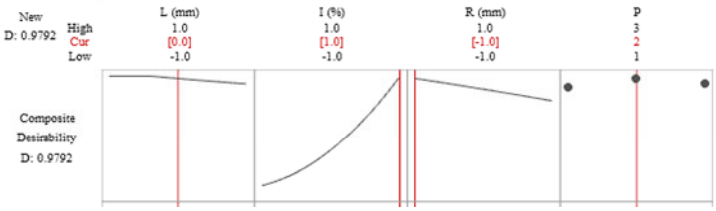

(a)

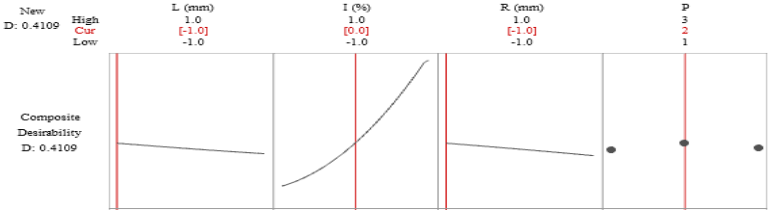

(b)

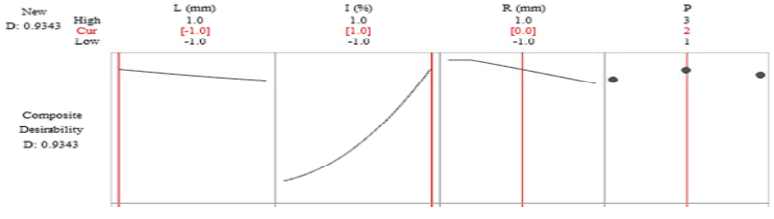

(c)

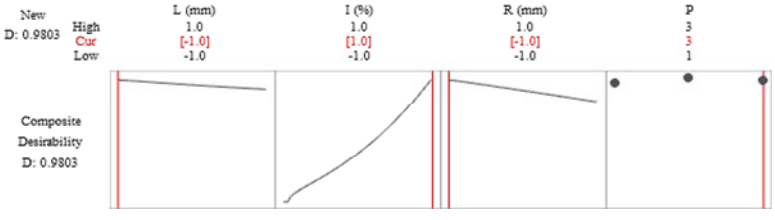

(d)

Figure 10 % reduction in compression and tensile strength with changing the optimal level (see online version for colours)

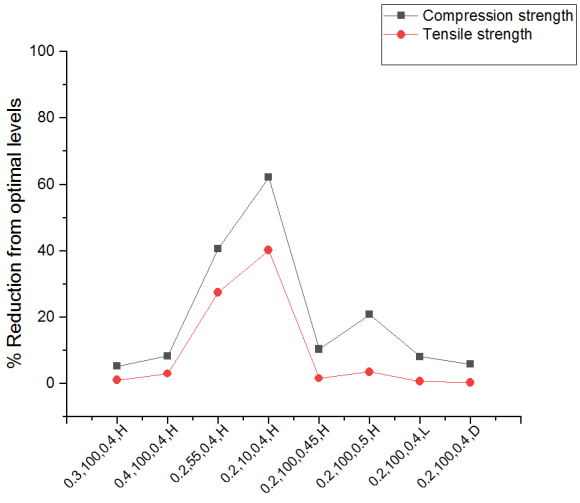

3.4 Stress-strain curve for tensile and compression

The compression and tensile stress versus strain and are analysed at optimised levels (i.e., 100% infill %, 0.1 mm layer height, raster width of 0.40 mm and hexagonal pattern) and also for the pattern types other than in optimised level (i.e., linear and diamond) for comparison. Figures 11(a) and 11(b) show that maximum compression and tensile strength obtained at optimal levels are 80 MPa and 38 MPa approximately with a percentage strain of 0.5%. It could be due to strong bonding on six sides of the hexagonal pattern providing a strong contact with the neighbour molecules (Tymrak et al., 2014). At lower layer heights, the bond between the layers got strengthened, and as a result, better mechanical strength can be achieved (Nugroho and Budiantoro, 2019). Similarly, the infill percentage represents the quantity of build material as the density increases; the mechanical strength also increases (Nugroho and Budiantoro, 2019).

Figure 11 Stress versus strain curve for (a) compression and (b) tensile (see online version for colours)

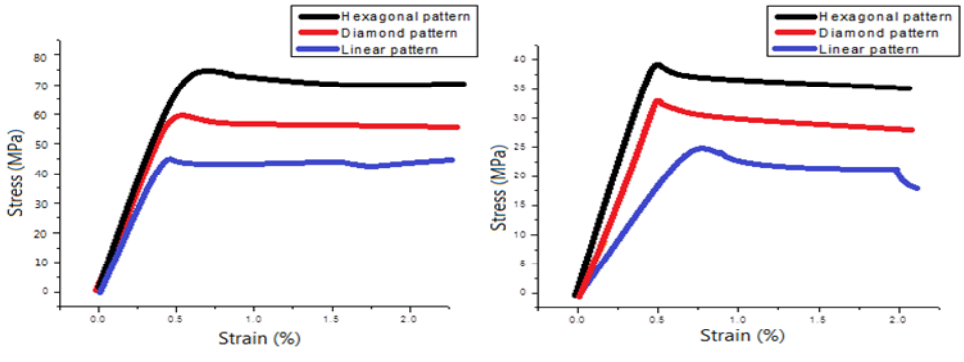

(a) (b)

4 Conclusions

The present study deals with the application of the categorical Box Behnken technique based on RSM to optimise the tensile and compression behaviour of PLA 3D printed parts. For this purpose, 45 experimental runs were conducted using a Box Behnken design based on the three levels' combination of process parameters. The input process parameters were layer height, infill percentage, raster width, and infill patterns (linear, hexagonal, and diamond), while the responses were tensile strength and compression strength. The three levels considered for layer height were 0.1, 0.2 and 0.3 mm, raster width were 0.40, 0.45, 0.50 mm and the infill percentages were 10%, 50% and 100% respectively. Specimens were printed according to ASTM D638 standards on the MakerBot desktop 3D printer. The ANOVA results revealed that the layer height, infill percentage, and raster width have a significant effect on tensile and compression strength. Infill pattern remains vital for tensile while insignificant for compression behaviour. Regression models are developed to study the effect of printing process parameters on compression and tensile strength. It revealed that compression and tensile strength for linear, hexagonal and diamond pattern could be improve significantly by increasing the infill % from 10% to 100%, however, decrease in strength is observed with increase in raster width from 0.4 mm to 0.5 mm. At the same time, the layer height has almost negligible effect on the compression strength, while tensile strength decreases with increase in layer height from 0.1 mm to 0.3 mm. Confirmation tests are performed to validate the effectiveness of the RSM technique. Finally, the optimised parameters obtained based on composite desirability function are layer height of 0.1 mm, infill percentage 100%, raster width of 0.40 mm and infill pattern is a hexagonal pattern. Stress vs. strain curves obtained at optimal levels shows that ultimate compression and tensile strength achieved are 75 MPa and 40 MPa. Finally, the results in the present provide useful technical information on FDM process parameters to improve the compression, and tensile of 3D printed parts.

References

Abid, S. et al. (2019) 'Optimization of mechanical properties of printed acrylonitrile butadiene styrene using RSM design', *The International Journal of Advanced Manufacturing Technology*, Vol. 100, Nos. 5–8, pp.1363–1372.

Anitha, R., Arunachalam, S. and Radhakrishnan, P. (2001) 'Critical parameters influencing the quality of prototypes in fused deposition modelling', *Journal of Materials Processing Technology*, Vol. 118, Nos. 1–3, pp.385–388.

Bagsik, A., Schöppner, V. and Klemp, E. (2010) 'FDM part quality manufactured with Ultem*9085', *Proceedings of International Conference Polymeric Materials*, pp.1–8.

Bellehumeur, C. et al. (2004) 'Modeling of bond formation between polymer filaments in the fused deposition modeling process', *Journal of Manufacturing Processes*, Vol. 6, No. 2, pp.170–178.

Box, G.E., Hunter, W.G. and Hunter, J.S. (1978) *Statistics for Experimenters*, Vol. 664, John Wiley and Sons, New York.

Camargo, J.C. et al. (2019) 'Mechanical properties of PLA-graphene filament for FDM 3D printing', *The International Journal of Advanced Manufacturing Technology*, Vol. 103, Nos. 5–8, pp.2423–2443.

Dawoud, M., Taha, I. and Ebeid, S.J. (2016) 'Mechanical behaviour of ABS: an experimental study using FDM and injection moulding techniques', *Journal of Manufacturing Processes*, Vol. 21, pp.39–45, https://doi.org/10.1016/j.jmapro.2015.11.002.

Equbal, A. et al. (2019) 'Multi-criterion decision method for roughness optimization of fused deposition modelled parts', in *Additive Manufacturing Technologies from an Optimization Perspective*, pp.235–262, IGI Global, Hershey, PA, USA.

Fernandez-Vicente, M. et al. (2016) 'Effect of infill parameters on tensile mechanical behavior in desktop 3D printing', *3D Printing and Additive Manufacturing*, Vol. 3, No. 3, pp.183–192.

Ferreira, S.C. et al. (2007) 'Box-Behnken design: an alternative for the optimization of analytical methods', *Analytica Chimica Acta*, Vol. 597, No. 2, pp.179–186.

Haleem, A., Javaid, M., Khan, S. and Khan, M.I. (2020) 'Retrospective investigation of flexibility and their factors in additive manufacturing systems', *International Journal of Industrial and Systems Engineering*, Vol. 36, No. 3, pp.400–429.

Hossain, M.S. et al. (2014) 'Improved mechanical properties of fused deposition modeling-manufactured parts through build parameter modifications', *Journal of Manufacturing Science and Engineering*, Vol. 136, No. 6:061002, https://doi.org/10.1115/1.4028538.

Izdebska, J. and Thomas, S. (2016) *Printing on Polymers: Fundamentals and Applications. Printing on Polymers: Fundamentals and Applications*. William Andrew, USA.

Kamoona, S.N., Masood, S.H. and Mohamed, O.A. (2018) 'Experimental investigation on flexural properties of FDM processed Nylon 12 parts using RSM', in *IOP Conference Series: Materials Science and Engineering*, IOP Publishing.

Kumar, S., Kannan, V.N. and Sankaranarayanan, G. (2014) 'Parameter optimization of ABS-M30i parts produced by fused deposition modeling for minimum surface roughness', *International Journal of Current Engineering and Technology*, Vol. 3, No. 3, pp.93–97.

Kumar, S., Yadav, R.N. and Kumar, R. (2020) 'Modelling and optimisation of duplex turning of titanium alloy (grade 5) using Taguchi methodology-response surface methodology', *International Journal of Industrial and Systems Engineering*, Vol. 35, No. 4, pp.463–481.

Kumar, V. et al. (2018) 'GA-based optimisation using RSM in WEDM of Nimonic-90: a nickel-based super alloy', *International Journal of Industrial and Systems Engineering*, Vol. 28, No. 1, pp.53–69.

Luzanin, O., Movrin, D. and Plancak, M. (2014) 'Effect of layer thickness, deposition angle, and infill on maximum flexural force in FDM-built specimens', *Journal for Technology of Plasticity*, Vol. 39, No. 1, pp.49–58.

Melenka, G.W. et al. (2015) 'Evaluation of dimensional accuracy and material properties of the MakerBot 3D desktop printer', *Rapid Prototyping Journal*, Vol. 21, No. 5, pp.618–627.

Mohamed, O.A., Masood, S.H. and Bhowmik, J.L. (2015) 'Optimization of fused deposition modeling process parameters: a review of current research and future prospects', *Advances in Manufacturing*, Vol. 3, No. 1, pp.42–53.

Murugan, R., Mitilesh, R. and Singamneni, S. (2018) 'Influence of process parameters on the mechanical behaviour and processing time of 3D printing', *International Journal of Modern Manufacturing Technologies*, Vol. 10, No. 1, pp.69–75.

Nugroho, A.W. and Budiantoro, C. (2019) 'Improving the tensile properties of 3D printed PLA by optimizing the processing parameter', *JEMMME (Journal of Energy, Mechanical, Material, and Manufacturing Engineering)*, Vol. 4, No. 1, pp.29–36.

Panda, B.N. et al. (2017) 'Performance evaluation of warping characteristic of fused deposition modelling process', *The International Journal of Advanced Manufacturing Technology*, Vol. 88, Nos. 5–8, pp.1799–1811.

Patel, P.B., Patel, J.D. and Maniya, K.D. (2015) 'Evaluation of FDM process parameter for PLA material by using MOORA-TOPSIS method', *International Journal of Mechanical and Industrial Technology*, Vol. 3, No. 1, pp.84–93.

Peng, A., Xiao, X. and Yue, R. (2014) 'Process parameter optimization for fused deposition modeling using response surface methodology combined with fuzzy inference system', *The International Journal of Advanced Manufacturing Technology*, Vol. 73, Nos. 1–4, pp.87–100.

Popescu, D. et al. (2018) 'FDM process parameters influence over the mechanical properties of polymer specimens: a review', *Polymer Testing*, Vol. 69, pp.157–166, https://doi.org/10.1016/j.polymertesting.2018.05.020.

Puigoriol-Forcada, J.M. et al. (2018) 'Flexural fatigue properties of polycarbonate fused-deposition modelling specimens', *Materials & Design*, Vol. 155, pp.414–421, https://doi.org/10.1016/j.matdes.2018.06.018.

Rajpurohit, S.R. and Dave, H.K. (2020) 'Prediction and optimization of tensile strength in FDM based 3D printing using ANFIS', in *Optimization of Manufacturing Processes*, pp.111–128, Springer, Cham, https://doi.org/10.1007/978-3-030-19638-7_5.

Rayegani, F. and Onwubolu, G.C. (2014) 'Fused deposition modelling (FDM) process parameter prediction and optimization using group method for data handling (GMDH) and differential evolution (DE)', *The International Journal of Advanced Manufacturing Technology*, Vol. 73, Nos. 1–4, pp.509–519.

Rohde, S. et al. (2018) 'Experimental characterization of the shear properties of 3D-printed ABS and polycarbonate parts', *Experimental Mechanics*, Vol. 58, No. 6, pp.871–884.

Shandilya, P., Jain, P. and Jain, N. (2012) 'Prediction of surface roughness during wire electrical discharge machining of SiCp/6061 Al metal matrix composite', *International Journal of Industrial and Systems Engineering*, Vol. 12, No. 3, pp.301–315.

Sood, A.K., Ohdar, R.K. and Mahapatra, S.S. (2010) 'Parametric appraisal of mechanical property of fused deposition modelling processed parts', *Materials & Design*, Vol. 31, No. 1, pp.287–295.

Sukindar, N.A. et al. (2017) 'Analysis on the impact process parameters on tensile strength using 3D printer repetier-host software', *Journal of Engineering and Applied Sciences*, Vol. 12, No. 10, pp.3341–3346.

Torres, J. et al. (2016) 'An approach for mechanical property optimization of fused deposition modeling with polylactic acid via design of experiments', *Rapid Prototyping Journal*, Vol. 22, No. 2, pp.387–404.

Trhlíková, L. et al. (2016) 'Study of the thermal properties of filaments for 3D printing', *AIP Conference Proceedings*, Vol. 1752, No. 1, p.040027, AIP Publishing LLC, USA.

Tymrak, B., Kreiger, M. and Pearce, J.M. (2014) 'Mechanical properties of components fabricated with open-source 3-D printers under realistic environmental conditions', *Materials & Design*, Vol. 58, pp.242–246, https://doi.org/10.1016/j.matdes.2014.02.038.

Wang, C.C., Lin, T.W. and Hu, S.S. (2007) 'Optimizing the rapid prototyping process by integrating the Taguchi method with the Gray relational analysis', *Rapid Prototyping Journal*, Vol. 13, No. 5, pp.304–315.

Zhang, J.W. and Peng, A.H. (2012) 'Process-parameter optimization for fused deposition modeling based on Taguchi method', in *Advanced Materials Research*, Vol. 538, pp.444–447, Trans Tech Publ., Switzerland, https://doi.org/10.4028/www.scientific.net/amr.538-541.444.